Numerical study of the moisture content threshold under prescribed burning conditions

Carmen Awad, Nicolas Frangieh, Thierry Marcelli, Gilbert Accary, Dominique Morvan, Sofiane Meradji, François Joseph Chatelon, Jean Louis Rossi

Numerical study of the moisture content threshold under prescribed burning conditions

Carmen Awad [a], Nicolas Frangieh [a,*], Thierry Marcelli [a], Gilbert Accary [b], Dominique Morvan [c], Sofiane Meradji [d], François Joseph Chatelon [a], Jean Louis Rossi [a]

[a] UMR CNRS SPE 6134, Université de Corse, 20250, Corte, France
[b] Scientific Research Center in Engineering, Lebanese University, Museum, 1106, Beirut, Lebanon
[c] Aix Marseille Université, CNRS, Centrale Marseille, M2P2, Marseille, France
[d] Laboratoire IMATH, EA 2134, Université de Toulon, 83160, Toulon, France

ARTICLE INFO

Keywords:
Fuel moisture-content threshold
Fire behaviour
Numerical simulation
Grassland fire
Prescribed burning
Numerical modelling

ABSTRACT

The safety during prescribed burnings could be achieved by conducting these operations under marginal conditions of fire propagation. This type of fire can or cannot propagate on account of small deviations of the burning conditions, mainly the wind speed, the fuel load, and the fuel moisture-content. In this context, numerical simulations of grassland fires were conducted under marginal conditions in order to relate the moisture-content threshold of propagation success to the wind speed and the fuel load. The simulations were conducted using FireStar2D, a complete physical 2D fire simulator based on a multiphase modelling approach. The 10 m-open wind speed ranged from 0 to 10 m/s and the fuel load varied from 0.1 kg/m^2 to 0.7 kg/m^2. The effects of wind speed and fuel moisture-content on the fire behaviour and on the flame parameters are discussed. The results show that the moisture threshold increases with the fuel load until it reaches a value beyond which there is no dependence. A similar dependence of the moisture threshold on the wind speed is also observed. Finally, empirical formulae were constructed to relate the fuel moisture content threshold to the wind speed and the fuel loading implicitly through Byram's convective number.

1. Introduction

Prescribed fires play an integral role in forest management and risk reduction. By definition, prescribed burning is a fire applied in a knowledge manner to forest fuels on a specific land area under selected weather conditions to accomplish predetermined, well-defined management objectives [1]. In fact, it's considered as one of the most effective method for land and plant managing communities and controlling natural succession [2]. It can be used for wide spectrum of objectives [3–8]. The most common application is the reducing wildfire hazard and the decreases of the intensity of a subsequent fire by the elimination of fuel loads accumulation, especially the finer elements, by disrupting the continuity of the fuel coverage [9], and by the creation of fuelbreaks [2]. Prescribed fires are also used to control the spread of aggressive plants, to reduce of plant diseases, to prepare sites for seeding and planting, and to improve wildfire habitat and manage endangered species [10,11].

Once ignited, the fire behaviour and intensity depend of the weather, topography, and fuels characteristics. So, in order to prevent harmful impacts on forests and to obtain low intensity fires, different burn techniques can be used depending on the angle of exposure of the unburned fuel to the flame [4,12]. The proper technique to use can change as these factors change. Atmospheric conditions should be favourable for smoke to rise and disperse into the upper air. Each method has strengths and weaknesses depending on the weather conditions, size of the area, and expertise of the operators conducting the fire.

Indeed, weather parameters have a large impact on prescribed burning and fire behaviour, specifically wind speed, temperature and relative humidity. Wind speed and direction control how fast and in which direction a fire will spread. Also, the unsteady nature of the wind flow (gusts) can have a significant impact on fire behaviour and spread [13]. For instance, in southern United States, the recommended wind speed ranges from 0.5 to 7 m/s (measured at 2 m above ground) [14]. Temperature must be considered for two reasons: high temperature has great influence on overstory vegetation and plays a great role in fuel moisture-content dynamics. On the other hand, the lower the relative humidity, the lower the fuel moisture-content and the more rapidly fuels

* Corresponding author.
E-mail address: frangieh_n@univ-corse.fr (N. Frangieh).

Nomenclature

B	Stefan-Boltzmann constant (W/m^2/K^4)
c_p	specific heat of vegetative fuel (J/kg/K)
c_{p0}	specific heat of ambient air (J/kg/K)
e	depth of fuel bed (m)
g	Earth acceleration (m/s^2)
I	fire line intensity (W/m)
LAI	Leaf Area Index
FMC	Fuel Moisture Content (mass of water/mass of dry mater)
m_x	fuel moisture content threshold that determine fire propagation (mass of water/mass of dry mater)
ROS	rate of spread (m/s)
s	surface area to volume ratio (1/m)
S_e	model universal constant
T	flame temperature (K)
T_a	ambient temperature (K)
T_i	ignition temperature (K)
U	wind speed (m/s)
Δh	latent heat of evaporation (J/kg)

Greek

ρ_ϖ	fuel particle density (kg/m^3)
ρ_0	ambient air density (kg/m^3)
β	solid fuel packing ratio
σ	solid fuel load (kg/m^2)
δ	extinction length (m)
τ	flame residence time (s)
τ_0	flame residence time parameter (75591 s/m)
τ_{opt}	critical optical thickness (m)

will dry. For example, the recommended range of relative humidity, in Indiana (United States), for prescribed burning is between 30 and 55% [10]. At the lower end of this range, prescribed burning can become dangerous as fire intensities increase. At the higher end, the fuel will burn with a low fire-line intensity to the point that the fire may not sustain or accomplish the desired objectives. Many studies showed that the success of the prescribed-fire spread depends not only on the wind speed but also on the physical properties of the vegetation, such as the fuel moisture-content and load [15–17]. Indeed, the fuel moisture content has a great effect on fire behaviour [18–21], and fire activities [16, 22]. In fact, fuel moisture content is a critical factor affecting the fire intensity, the amount of consumed fuel, the combustion rate [23], and the rate of spread [18,20,24]. Also, the fuel moisture content decreases the flame temperature [19,25] and dilutes the oxygen in the combustion area [26]. King [27] showed that the released water vapour decreases soot concentration, and decreases consequently the flame emissivity and the radiant heat. Other studies showed that the fuel moisture content has a critical threshold that determines fire extinction [9,28,29]. Rothermel [9] showed that fire does not spread in Pinus ponderosa needles bed when the fuel moisture content is above 30%. Morvan [18] numerically showed that grassland fires do not spread under weak wind conditions if the fuel moisture content is higher than 20%. Trabaud [30] estimated that the fuel moisture content of extinction for the Mediterranean shrubs is about 32%. Models that evaluate the fuel moisture-content threshold of extinction are rare; the most known is the model proposed by Wilson [29] that relates the fuel moisture threshold of extinction to the vegetation structure. Most of these studies were conducted without considering the effect of wind speed on the upper limit moisture for which the fire spreads. In fact, other studies showed higher extinction values of fuel moisture content when including the effect of wind speed. Marsden-Smedley et al. [16] had shown that the upper limit of FMC of fire propagation in button moorlands can reach 76% when the wind speed is higher than 2 km/h. Valdivieso et al. [31] conducted several tests using pine needles fuel beds under controlled wind conditions and they found that the fuel moisture content of extinction increases from 54% to 140% when the wind speed increases from 0.5 m/s to 5 m/s. They also proposed an empirical model that relates the moisture content threshold of extinction to the wind speed but without considering the fuel properties. However, most of the models that determine the fire propagation success based on both wind speed and fuel properties are probability functions [15,17] constructed from experimental tests. These models do not lead to accurate values of the extinction conditions. Balbi et al. [28] proposed an analytical model that determines the fuel moisture threshold based on fuel properties and on ambient temperature. This model can be applied for all type of vegetation, under no slope and weak wind conditions. The effectiveness of Balbi's analytical model in predicting the FMC threshold has been tested [32] using experimental and numerical data. In this study, laboratory fire experiments were carried out in excelsior fuel beds, while the numerical simulations were conducted using the complete physical fire model "FireStar2D" [33–35] for a homogeneous grassland and heterogeneous (shrub) fuel bed. This study showed that the predictions of Balbi's model of the FMC threshold for calm wind conditions (up to 0.5 m/s) are in fairly good agreement with the experimental data and the numerical results obtained using FireStar2D.

Following on from the previous study [32], the present study is motivated by the limitation of Balbi's model (and the absence of other operational models) in predicting the FMC threshold under active wind conditions. Consequently, the aim of this study is to numerically determine the required fuel properties (fuel load and moisture content) for a successful prescribed burning on leveled ground. For this purpose, several numerical simulations of grassland fires were conducted using the complete physical model FireStar2D in order to relate the FMC threshold of extinction to the wind speed and to the fuel load. In the process, the study describes the effects of wind speed and the FMC on fire behaviour (fire regime and flame parameters). These effects have already been addressed in the literature using FireStar2D model for calm and moderate wind speeds [18,32]. These studies and many others [13, 33–36] have highlighted the predictive potential of FireStar2D model in addressing the effects of the wind conditions, the fuel properties (FMC and fuel load), and other parameters (slope, fuel break, wind unsteadiness …) on fire behaviour.

Finally, in a recent thematic report [37], the United Nations Office for Disaster Risk Reduction (UNDRR) stressed the importance of better inclusion of science and technology in Disaster Risk Reduction efforts. As in many other fields of science, the development of new fire simulation tools to have more insight on the underlying physics, is considered nowadays to be a promising approach. At a large scale, these tools aim to predict the fire behaviour [38,39] and the trajectory of a fire front through a landscape, while at a smaller scale, they aim to describe the details of the interaction between the flames and potential targets (industries, vegetation, houses …) [38,40,41]. Indeed, the (UNDRR) report [37] highlighted that the main challenge for the next decades may be to close the gap between stakeholders' needs and scientific knowledge and tools. In this context, the present numerical study could be seen as a further modelling effort to give insights into thresholds that can lead to successful burns and how to adjust timing and ignition techniques to overcome extinction in marginal conditions and prevent propagation in dangerous conditions.

2. Physical considerations and mathematical model

As mentioned and argued for in introduction, 2D numerical simulations were conducted using a complete physical fire model, namely

FireStar2D. The mathematical model used in FireStar2D is based on a multiphase formulation [42], it consists in a first step in space-averaging the conservation equations (mass, momentum, energy …) governing the behaviour of the coupled system formed by the vegetation and the surrounding atmosphere. This averaging is performed on elementary control volumes including both the solid phase (the vegetation) and the gaseous phase. The model consists of two parts that are solved on two distinct grids. The first part consists of the equations of a reacting turbulent flow in the gaseous phase composed as a mixture of fresh air with the gaseous products resulting from the degradation of the solid phase (by drying, pyrolysis, and heterogeneous combustion) and the homogeneous combustion in the flaming zone. The second part consists of the equations governing the state and the composition of the solid phase subjected to an intense heat flux coming from the flaming zone.

Solving the gaseous phase model consists in the resolution of conservation equations of mass, momentum, energy (in enthalpy formulation), and chemical species (O_2, N_2, CO, CO_2, and H_2O) filtered in time using an unsteady RANS approach (URANS), with Favre average formulation [43]. The closure of the averaged conservation equations is based on the eddy viscosity concept [44] obtained from an evaluation of the turbulent kinetic energy k and its dissipation rate ε. In the URANS approach, a high Reynolds number version of a two-equation statistical turbulence model (k-ε) is used with the RNG formalism [45,46]. A combustion model based on Eddy Dissipation Concept (EDC) [44,47] is used to evaluate the combustion rate occurring in the gaseous phase. Finally, because radiation heat transfer (mainly due to the presence of soot particles in the flames) plays an important role for the propagation of the fire front, the field of soot volume-fraction in the gas mixture is calculated by solving a transport equation [48] including a thermophoretic contribution in the convective term and taking into consideration soot oxidation [49].

Concerning the solid phase model, during the thermal degradation, the composition of the solid fuel particles representing the vegetation is represented as a mixture of dry material, charcoal, moisture, and residual ashes. For each solid particle, the model consists in solving the equations governing the time evolutions of the mass fractions of water, of dry material, of charcoal, as well as of the total mass of the solid particle, its volume fraction and its temperature. The degradation of the vegetation is governed by three temperature-dependent mechanisms: drying, pyrolysis, and charcoal combustion [35,42,50]. The pyrolysis process starts once the drying process is completed and charcoal combustion starts once the pyrolysis process is achieved. The constants of the model associated with the charcoal combustion (activation energy and pre-exponential factor) are evaluated empirically from a thermal analysis conducted on various solid fuels samples [42,51].

The interaction between the gaseous phase and the solid one is taken into account through coupling terms that appear in both parts of the model. These terms are linearly interpolated between the fluid-phase and solid-phase grids. The coupling in the momentum and turbulence equations is obtained by adding aerodynamic drag terms [52] Heat transfer between the gas mixture and the solid fuel is based on empirical correlations for convective transfer coefficient [51]. Finally, mass transfer from the solid phase to the gaseous phase is represented by adding source/sink terms in the mass conservation equations of both phases. The set of transport equations in the gas phase are solved using an implicit finite Volume (FV) method [53,54]. To avoid the introduction of false numerical diffusion, the Ultra-Sharp (Universal Limiter for Tight Resolution and Accuracy Resolution Program) has been adopted [55]. The Radiative Transport Equation (RTE) is solved using a Discrete Ordinate Method (DOM), consisting of the decomposition of the radiation intensity in a finite number of directions [56]. The interaction between turbulence and radiation is formulated using an optically thin fluctuation approximation (OPFA) [18,34,36,57]. The set of ordinary differential equations describing the time evolution of solid-fuel state (mass, temperature, and composition) are solved separately using a fourth order Runge-Kutta method.

The details of FireStar2D model have been thoroughly described in previous publications, we invite the reader to consult references [33,35,58,59] for more information about this 2D model and for a comparison with other wildfire tools available in the community.

The simulations were performed in a 2D domain, 170 m long and 35 m height, as shown in Fig. 1. A homogenous layer of Australian grassland, whose physical properties are described in Table 1, lied between x = 20 m and x = 170 m. Different fuel loads are considered in this study by changing the fuel height between 0.1 and 0.7 m and maintaining the same fuel density and packing ratio. Ignition was obtained by instantaneous injection of CO at 1600 K from the ground (between x = 20 m and x = 22 m) during 5 s and with a constant velocity of 1 m/s. Ignition is activated after reaching a statistically-steady profile of the turbulent boundary-layer inside and above the fuel bed [36], which required 30 s of simulation time.

In order to insure accurate simulation results, the mesh size must respect physical and numerical criteria related to the fuel-bed depth (e) and the characteristic length of radiation extinction within the vegetation (δ) given by Eq. (1), i.e.: $\Delta x < \delta$ and $\Delta z < \min(e/4, \delta)$.

$$\delta = {}^{4}/_{s\beta} = 0.5 \ \text{m} \qquad \text{(Eq. 1)}$$

The wind velocity profile is described by a logarithmic function imposed at the left boundary of the computational domain. The wind speed was given at 10 m above the ground level and ranged between 1 and 10 m/s.

3. Results and discussion

As mentioned in the introduction, the main objective of this study is to relate the FMC threshold that determine a fire-spread success to the wind speed and the fuel load. A propagation was considered successful if the fire spreads over more than 50 m from ignition point and reaches a constant rate of spread (ROS). For a FMC equal to the extinction threshold, denoted m_x, most of the simulated fires spread over 15–30 m before extinction. This transitional phase is directly related to the ignition method, where the burner is activated during 5 s, which maintains the fire spread over some distance before extinction. For instance, Fig. 2 shows the trajectory of the pyrolysis front obtained under marginal conditions for $U_{10} = 4$ m/s and e = 0.5 m ($\delta = 0.5$ kg/m^2); we clearly notice fire extinction for FMC = 149% while steady fire spread was obtained for FMC = 148% allowing ROS calculation. For all considered cases, the FMC extinction threshold-value, m_x, was determined within 1% error; in the case of Fig. 2, $m_x = 149\%$.

3.1. Effects of the wind speed and of the FMC on fire behaviour

Fig. 3a shows the FMC threshold (m_x) as a function of the 10-m open wind speed for different vegetation fuel loads. For low to moderate U_{10} values (up to 6 m/s), m_x increases quasi-linearly with the wind velocity before reaching an asymptotic value for $U_{10} > 6$ m/s where no noticeable variation of m_x is visible for the fuel loads. Similarly, Fig. 3b shows that m_x increases with the fuel load before reaching an asymptotic value for $\sigma > 0.5$ kg/m^2, beyond which the dependence of m_x on the fuel load becomes relatively weak.

And wind-driven fires. Byram's convective number given by Eq. (2) is often used in the literature [26] to characterise wildfires behaviours; this dimensionless number represents the power ratio of the two forces governing the flames direction and consequently the propagation of a wildfire: the buoyancy force due to temperature difference (and therefore density) between the hot plume above the fire and the ambient air, and the inertia force due to the wind. In Eq. (2), I is the fire line intensity (W/m), g is Earth gravity, and subscript 0 refers to ambient-air physical properties. Plume-dominated fires are obtained for large values of Byram's convective number (typically for $N_C > 10$), while wind-dominated fires are obtained for small values of N_C (typically for

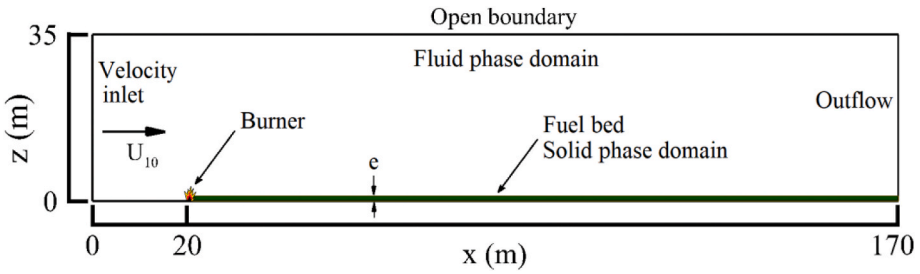

Fig. 1. Computational domain and boundary conditions used in the 2D simulations of grassland fires.

Table 1
Physical properties of the homogenous fuel-bed layer.

Fuel particle density, ρ_v (kg/m^3)	500
Fuel packing ratio, β	0.002
Fuel moisture content, FMC (%)	5–200
Fuel depth, e (m)	0.1–0.7
Fuel load, σ (kg/m^2)	0.1–0.7
Surface-area to volume ratio, s (m^{-1})	4000

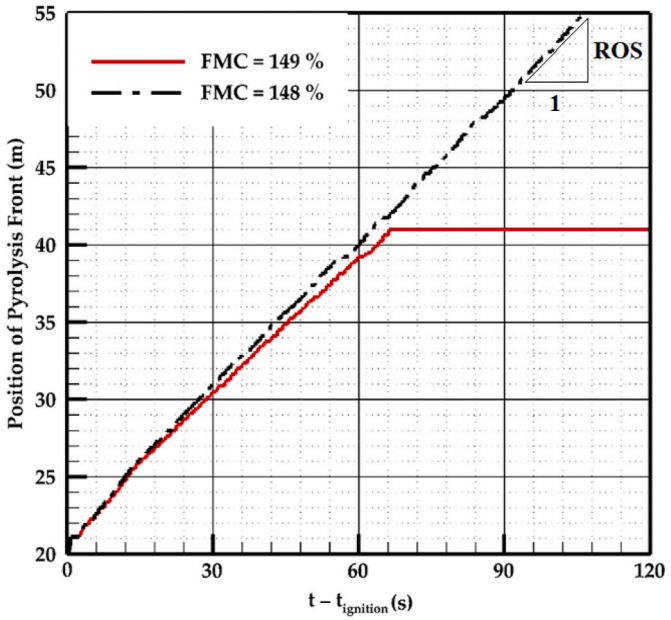

Fig. 2. Time evolution of the pyrolysis front position obtained under marginal conditions for U_{10} = 4 m/s and e = 0.5 m (δ = 0.5 kg/m^2). The ROS is the curve slope obtained at steady fire spread.

$N_C < 2$) [26].

$$N_C = \frac{2gI}{\rho_0 C_{P0} T_a (U_{10} - ROS)^3} \quad \text{(Eq. 2)}$$

Byram's convective number N_C is a decreasing function of the wind speed U_{10} [38] as well as of the FMC [18]; consequently, a combined increase of U_{10} and of FMC harshly reduces the power of the buoyancy force and the thermal plume direction becomes more affected by the wind that tilts the flame towards the vegetation cover and increases its length. These phenomena are illustrated in Figs. 4 and 5 that show the gas temperature field (i.e. flame) for a low and moderate wind speed (U_{10} = 2 and 4 m/s) and for two FMC values (5 and 90%). The colour bar indicates the temperature level of the gas while the arrowheads on the streamlines symbolize the wind stream direction.

For $U_{10} \leq 6$ m/s, all the simulated fires with a low FMC value (5%),

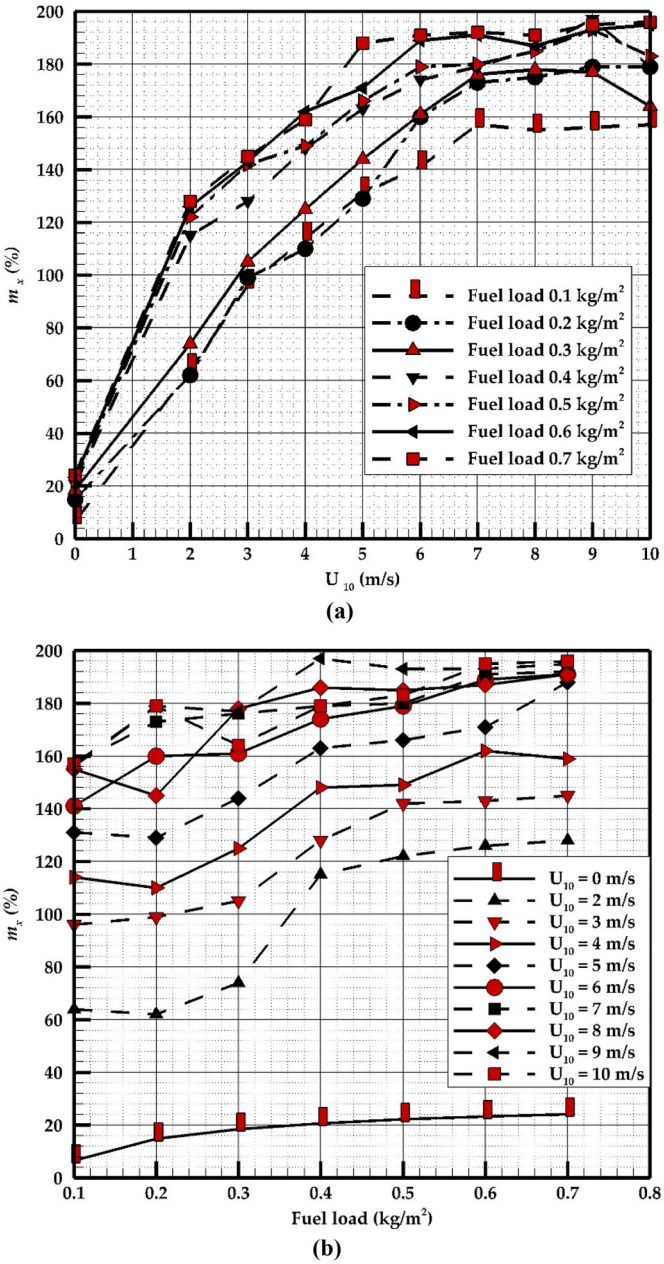

Fig. 3. Fuel moisture content threshold of fire extinction through a uniform grassland obtained for (a) different 10-m open wind speeds and (b) different fuel-bed loads.

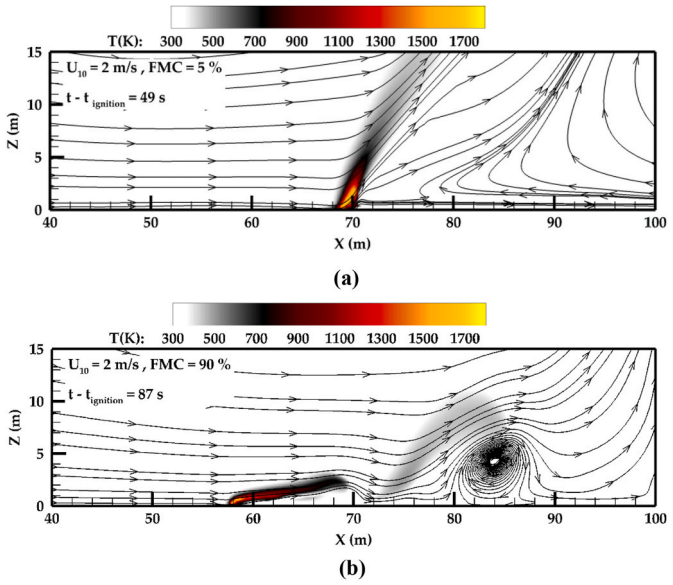

Fig. 4. Temperature field and resulting flow velocities (in x and z directions) streamlines obtained for U_{10} = 2 m/s, for e = 0.5 m (δ = 0.5 kg/m^2), and for two values of FMC: (a) FMC = 5%, (b) FMC = 90%.

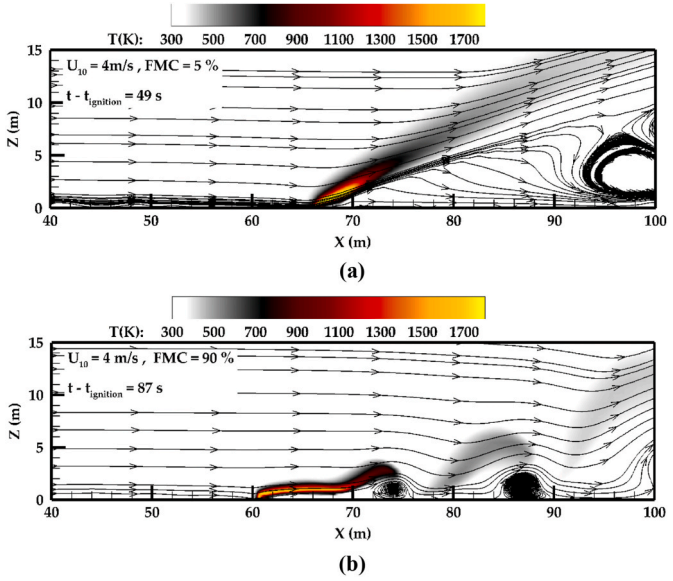

Fig. 5. Temperature field and resulting flow velocities (in x and z directions) streamlines obtained for U_{10} = 4 m/s, for e = 0.5 m (δ = 0.5 kg/m^2), and for two values of FMC: (a) FMC = 5%, (b) FMC = 90%.

for all considered fuel-load values, were plume-dominated fires or had a hybrid propagation regime between plume-dominated Figs. 4a and 5a show how an increase of the wind speed (from 2 to 4 m/s) significantly affects the rise of the flame by pushing it toward the unburned vegetation; this, results also in a significant increase of the flame depth. We notice also for both wind speeds, that when the FMC increases, the flame temperature decreases as well as the power of the buoyancy force; consequently, the flame becomes more affected by the wind speed action: the flame length increases and it leans toward the unburned vegetation.

Fig. 6 shows the profiles of the gas temperature and of the mass fraction of oxygen and water vapour, evaluated at the surface of the vegetation cover for FMC = 5% and 90%. We notice first that the flame temperature decreases as the FMC increases since a part of the energy is

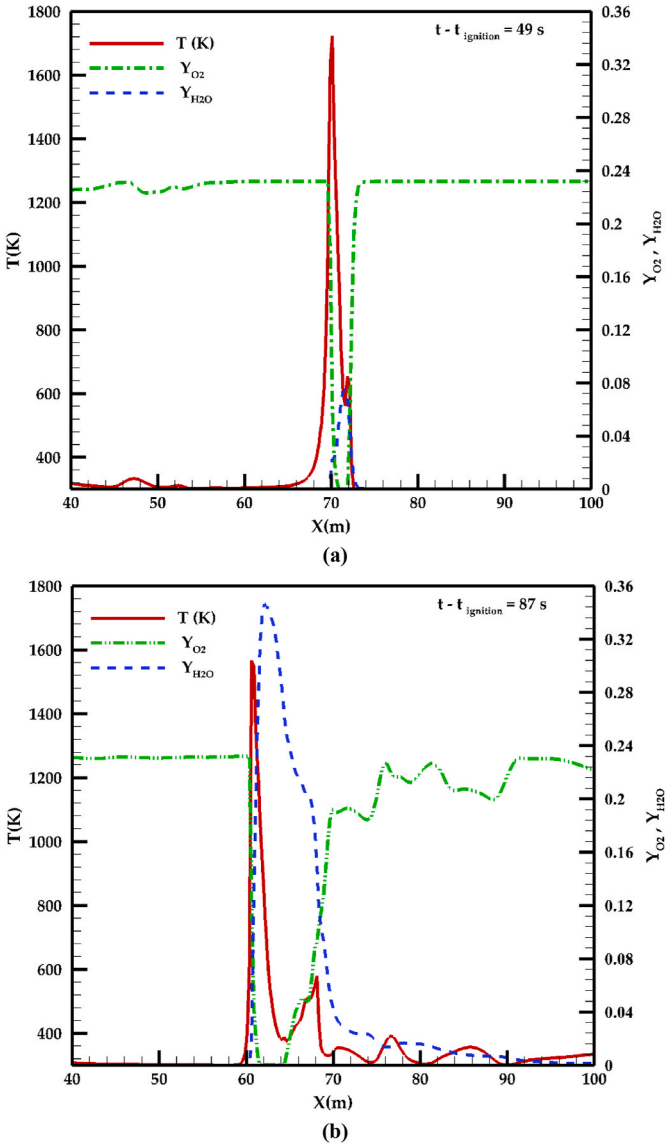

Fig. 6. Profiles of the gas temperature and the mass fraction oxygen and water vapour in the gas mixture, obtained at the surface of the vegetation cover (z = e) for e = 0.5 m (W = 0.5 kg/m^2), for U_{10} = 4 m/s, and for two values of FMC: (a) FMC = 5%, (b) FMC = 90%.

consumed for water vaporisation, and of course much more water vapour is transferred into the gaseous phase as the FMC increases. But Fig. 6 also shows the larger inclination of the flame for FMC = 90% and it leans onto the vegetation cover, which boosts the preheating of the unburned vegetation many meters beyond the combustion zone, up to a distance where the flame cannot sustain fire propagation. On the other hand, as the FMC increases, the larger amount of water vapour produced by vaporisation decreases oxygen concentration in the gas mixture (as shown in Fig. 6b) behind the flame, which can cause fire extinction when the FMC reaches it threshold value.

For U_{10} = 7 m/s most of the simulated fires with FMC = 5% were wind driven, i.e. $N_C < 2$ or very close to 2. For these fires ($U_{10} \geq 7$ m/s), the flame lengths are already important before increasing the wind speed or the FMC. As shown by Figs. 7 and 8, the increase of the wind speed or the FMC has again the effect of tilting the flame toward the vegetation cover and decreasing consequently the flame height. This results in reducing the size of the coherent structures observed downstream of the fire.

In the light of the analysis made so far, the asymptotic behaviour of

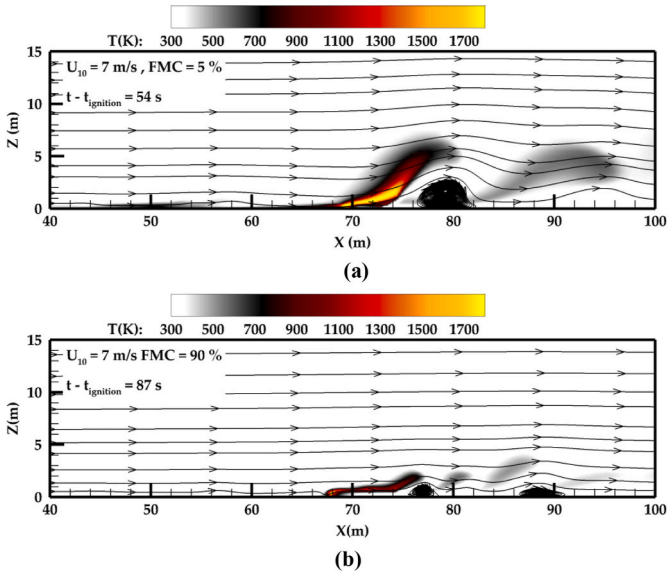

Fig. 7. Temperature field and resulting flow velocities (in X and Z directions) streamlines obtained for U_{10} = 7 m/s, for e = 0.5 m (δ = 0.5 kg/m^2), and for two values of FMC: (a) FMC = 5%, (b) FMC = 90%.

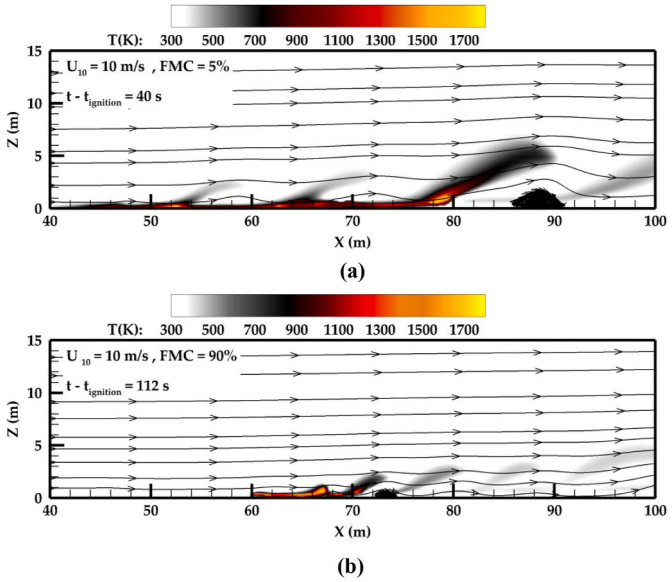

Fig. 8. Temperature field and resulting flow velocities (in x and z directions) streamlines obtained for U_{10} = 10 m/s, for e = 0.5 m (δ = 0.5 kg/m^2), and for two values of FMC: (a) FMC = 5%, (b) FMC = 90%.

the FMC threshold of extinction versus the wind speed can be explained as follows: m_x asymptotic values are relatively high (between 155% and 200% for the considered fuel loads, see Fig. 3a). At such high FMC values, the flame buoyant power is very weak because (1) a large amount of the heat release is for water vaporisation, (2) the large amount of water vapour drastically reduces the concentration of oxygen in the gas mixture behind the flame. Because the flame is very weak, the action of the wind speed on the flame geometry (mainly its length and tilt angle) reaches its full effect at moderate wind speeds (5–7 m/s according to the fuel load, see Fig. 3a). In other words, increasing the wind speed beyond the value for which the asymptotic value of m_x is reached does not affect the flame characteristics anymore, in a way that would increase heat transfer to the unburned vegetation.

3.2. Fuel-bed load effect on the FMC threshold of extinction

Previous studies showed that the fuel load has impact on fire behaviour, especially on the rate of spread and on fire sustainability [35, 40–42]. In fact, the fuel load or the depth of the fuel bed is a factor that determines whether the fire front is propagating in thin or thick mode through the fuel bed assimilated to a porous medium [58,60]. In this study the authors demonstrated that below some fuel thickness, the propagation velocity is inversely proportional to the fuel thickness (thermally thin mode). Above, this threshold thickness, the rate of spread tends towards a constant value (optically thick mode). This fire propagation mode depends on a critical optical thickness, given by Eq. (3), beyond which the vegetation medium is considered to be thick [58].

$$\tau_{opt} = s\beta e/4 \qquad \text{(Eq. 3)}$$

Fig. 3b shows that m_x increases with the fuel loading (up to 0.5 kg/m^2) until reaching a value beyond which the dependence of the fuel load becomes relatively weak. This behaviour change can be related to the fire propagation mode in the porous medium. For a relatively thin vegetation medium (τopt < 1) obtained for e < 0.5 m that also corresponds to σ < 0.5 kg/m^2, all the fuel-bed depth participates to the fire propagation; in this case, m_x increases with the fuel load. But, for a thicker vegetation medium, radiative heat transfer does not penetrate effectively the entire fuel-bed depth, and the lower fuel-bed layers are not heated enough to effectively participate to fire propagation [61]; m_x becomes less sensitive to the fuel load in this case. Indeed, as shown by Fig. 9, the radiative heat flux received by the lower part of the unburned vegetation (0.1 m above ground), located 1 m downstream of the flame, decreases substantially with the fuel-bed load. We also notice a change in the dependence of the radiative heat flux on the fuel load as the vegetation approximately reaches the critical optical thickness.

3.3. Empirical law for the FMC threshold of extinction

The prescribed fire success is usually predicted using statistical functions deduced from experimental tests using a specific vegetation [5,15,16]. These probability functions show that the fire sustainability depends of the fuel properties and weather conditions. The 70 points shown in Fig. 3 were used to construct the empirical relation of the FMC threshold of grassland-fire extinction, for a wind speed U_{10} ranged from 1 to 10 m/s and for a fuel load σ ranged from 0.1 to 0.7 kg/m^2. The least-square fitting of the 70 data points, using "Levenberg-Marquart"

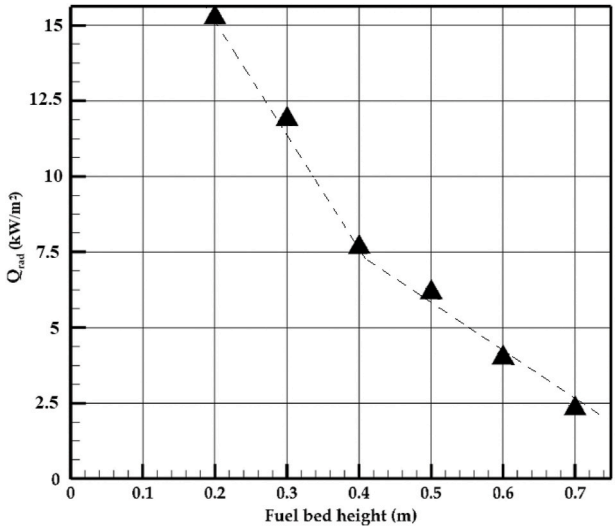

Fig. 9. Radiative heat flux received by the vegetation at point (70 m, 0.1 m) obtained for U_{10} = 2 m/s, FMC = 10%, and different fuel loads, when the flame was located at x = 69 m.

algorithm [62] results in the empirical relation given by Eq. (4), where the fuel load σ is expressed in kg/m^2 and the wind speed in m/s. m_{x0} is the FMC threshold of extinction, given by Eq. (5), obtained from an algebraic physical model proposed by Balbi et al., in 2014 [28] under no-wind conditions. In Eq. (5), Se = 0.47 is a universal constant, LAI = β. s.e/2 is the leaf area index, ρ_v is the fuel particle density, B is the Stefan-Boltzmann constant, cp is the vegetative fuel specific heat, Δh is the latent heat of evaporation, T is the mean flame temperature, T_i and T_a are respectively the ignition and ambient temperatures, $\tau_0 = 75591$ s/m is the flame residence time parameter [63] and *n* is the optical thickness parameter [64]. The proposed correlation approximates the simulations results with a coefficient of determination $R^2 = 0.977$.

$$m_x - m_{x0} = 46.53\sigma^{1.765} + 58.83U_{10}^{0.445} \quad \text{(Eq. 4)}$$

$$m_{x0} = \frac{\tau_0 B T^4}{n\rho_v \Delta h}\left(1 - \frac{S_e}{\sqrt{2LAI}}\right) - \frac{c_p(T_i - T_a)}{\Delta h} \quad \text{(Eq. 5)}$$

3.4. *Effects of the wind speed and of the FMC on the flame characteristics*

Fig. 10 shows the FMC dependence of the flame residence time τ_{Fire}. For $U_{10} \geq 4$ m/s, we clearly notice that the curves can divided into two parts: τ_{Fire} decreases with the FMC up to FMC = 30–40%, and then it increases for higher FMC values. This dependence has also been reported in the literature [18] for a fuel-bed depth e = 0.7 m using FireStar2D model. For the smallest wind speed ($U_{10} = 1$ m/s), only the first part of the curve (with a sharpest slope) can be observed, because the FMC threshold of extinction is too low to reach the part where τ_{Fire} increases with the FMC. To understand this behaviour, Byram's convective number N_C, given by Eq. (2), is represented versus the FMC for $U_{10} = 1$ and 4 m/s in Fig. 11. For $U_{10} = 1$ m/s, N_C decreases with the FMC and the last successfully propagating case, before reaching the extinction threshold occurs for FMC = 20%, results in $N_C = 1047$. Consequently, for $U_{10} = 1$ m/s, fire propagation regime is plume-dominated for all considered FMC values, and the air diluted by the vaporized water is drawn from the vicinity of the fire front into the flaming zone, which weakens the flame intensity until extinction for a FMC >20%. For $U_{10} =$ 4 m/s, NC decreases from 22.1 (plume-dominated fire) for FMC = 10%, to reach Nc = 10 for a FMC = 40%, which corresponds to the transition from a plume-dominated to a wind-driven fire. For FMC >40%, Nc

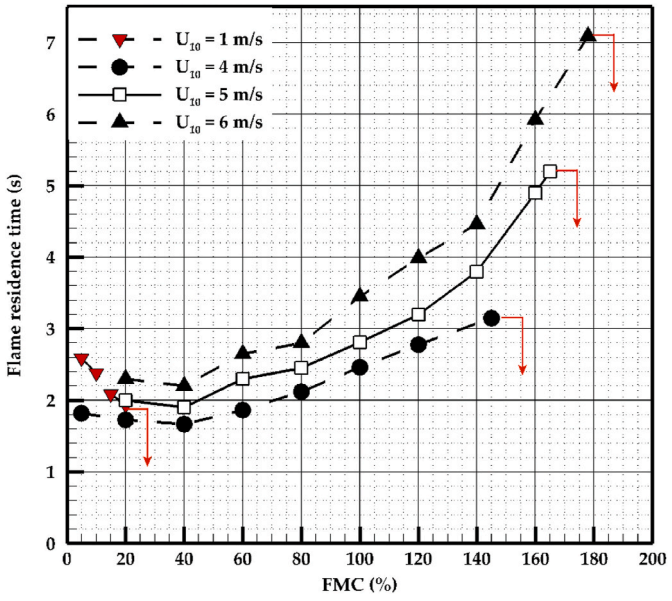

Fig. 10. Fire residence time versus the FMC, obtained for a fuel-bed thickness e = 0.5 m (W = 0.5 kg/m^2) and for different wind speeds. The vertical arrow indicates the FMC threshold of extinction.

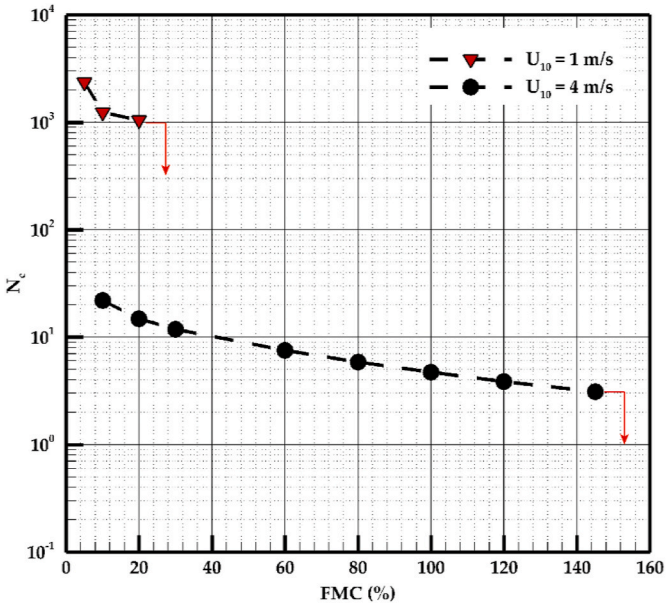

Fig. 11. Byram's convective number versus the FMC, obtained for a fuel-bed thickness e = 0.5 m (W = 0.5 kg/m^2) and for $U_{10} = 1$ and4 m/s. The vertical arrow indicates the FMC threshold of extinction.

continues decreasing and the fire behaviour becomes more wind driven, and vaporized water is better evacuated away from the flaming zone by the action of the cross wind. This fire-regime transition for $U_{10} = 4$ m/s could explain the dependence of the flame residence time on the FMC observed in Fig. 10. This behaviour change, where vaporized water is drawn into the flaming zone in plume-dominated regimes and evacuated away from it in wind driven regimes, can be clearly illustrated by the distributions of the water vapour fraction shown in Fig. 12 and corresponding to Figs. 4a and 5b. We notice that for $U_{10} = 2$ m/s and FMC = 5% (Fig. 12a), there is no water vapour downstream of the flaming zone because it has been drawn into it by the back flow. While for $U_{10} = 4$ m/s and FMC = 90% (Fig. 12b), water vapour is clearly being evacuated away from the flaming zone. The increase of the flame residence time, τ_{Fire}, observed for FMC >40%, also explains the dependence of the flame depth (equal to ROS × τ_{Fire}) on the FMC shown in Fig. 13. It is well

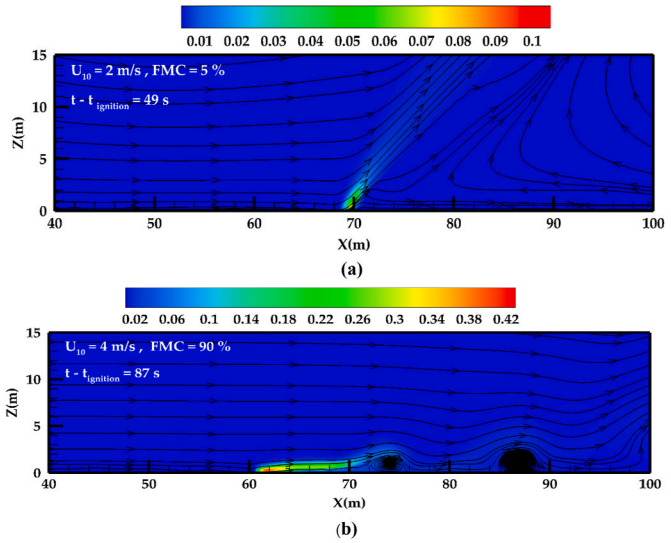

Fig. 12. Distribution of water-vapour mass-fraction and flow streamlines obtained (a) for $U_{10} = 2$ m/s, FMC = 5%, and e = 0.5 m, and (b) for $U_{10} = 4$ m/s, FMC = 90%, and e = 0.5 m.

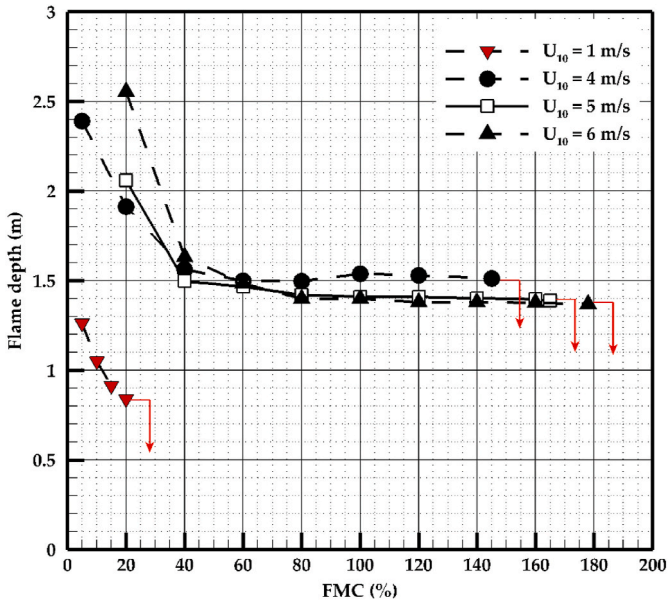

Fig. 13. Flame depth versus the FMC, obtained for a fuel-bed thickness e = 0.5 m (W = 0.5 kg/m^2) and for different wind speeds. The vertical arrow indicates the FMC threshold of extinction.

known that the ROS is always a decreasing function of the FMC [18,20]. Fig. 13 highlights clearly that flame depth decreases sharply for FMC values smaller than 40% because both the ROS and the flame residence time (τ_{Fire}) decrease. For larger values (FMC > 40%), the flame depth is practically independent of the FMC, and this results from the opposite actions of the FMC on the ROS and on the flame residence time; indeed, in this case τ_{Fire} increases with the FMC while the ROS always decreases.

3.5. Non-dimensional scaling of the FMC threshold of extinction

In order to remove the dimensional dependence of the FMC threshold relationship, given by Eq. (4), Byram's convection number N_C was evaluated using Eq. (2) for all successfully propagated fires, and the FMC is plotted in Fig. 14 versus the inverse of N_C. Fires with $1/N_C < 0.1$ are typically plume dominated, while fires with $1/N_C > 0.5$ are wind driven. The green symbols correspond to the marginal cases, for which increasing the FMC by 1% stops fire propagation, i.e. the FMC threshold of extinction m_x is reached. The marginal cases, defining the upper FMC boundary of successful fires, can be scaled with the inverse of Byram's convection number according to Eq. (6), were ln is the natural logarithm.

$$FMC_{marg}(\%) = 144 + 15.5\ \ln\left({}^{1}/_{N_C}\right) \qquad \text{(Eq. 6)}$$

Due to data scattering about the scaling law (see Fig. 14), Eq. (6) is less accurate than the empirical law given by Eq. (4) where a 0.977 coefficient of determination was achieved. It allows however to extend the prediction of the FMC threshold of extinction beyond the range of physical parameters (fuel load, wind speed, fuel properties) considered in this study. It covers a wide range of fire behaviours ($0.05 < N_C < 2500$), it requires however an estimation of the fire intensity and the ROS in order to predict the FMC threshold of extinction.

4. Conclusions

In order to understand how the fuel moisture content (FMC) characterizing a homogeneous grassland can determine a fire spread success on a flat terrain in prescribed wind conditions, 2D numerical simulations were conducted using a complete physical multiphase model

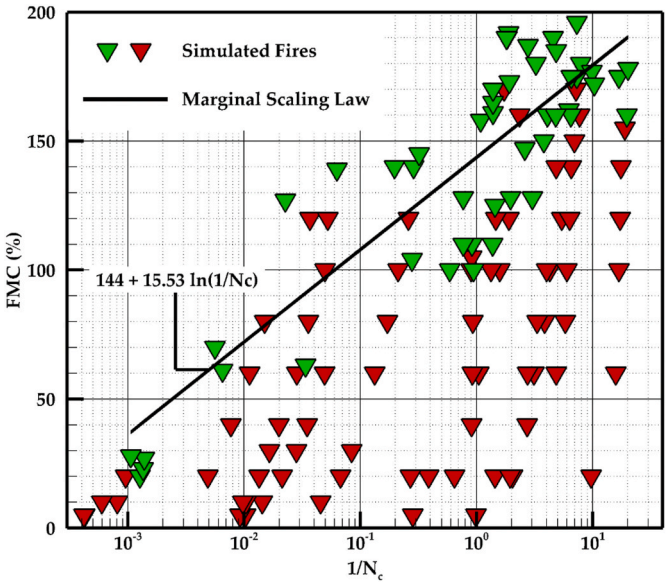

Fig. 14. FMC versus the inverse of Byram's convection number. The green symbols correspond to the marginal cases, for which increasing the FMC by 1% stops fire propagation, and the red symbols refer to the simulated cases where the fire front reaches the end of the domain. (For interpretation of the references to colour in this figure legend, the reader is referred to the Web version of this article.)

(FireStar2D) for different wind speeds and fuel loads.

The study showed that the FMC threshold of extinction m_x increases with the wind speed and the fuel load until reaching an asymptotic value beyond which m_x dependence on the wind speed and the fuel load fades away. The study also highlighted the combined effect of the wind speed and the FMC on fire behaviour, especially on the flame characteristics. Increasing the FMC reduces the flame intensity and makes the flame and the fire plume more vulnerable to the action of the cross wind. The FMC threshold of extinction was accurately correlated to the wind speed and to the fuel load; this explicit correlation allows to determine the marginal conditions for a successful prescribed-burning in terms of fire parameters that could be directly measured in the field. A scaling law was also proposed between the marginal FMC for a successful fire spread and Byram's convective number; this law extends the predictability of the FMC threshold of extinction beyond the physical parameters considered in this study, but requires however an estimation of the fire line intensity and of the ROS.

Many other fundamental aspects of prescribed fire under marginal conditions are not well understood and should be investigated, such as the impact of the unsteady nature of the wind flow due to gusts, the role played by the field slope under marginal conditions, and the competition between the wind and the slope when their directions are not aligned. Nevertheless, this study is a further step towards a better understanding fire behaviour under marginal conditions and more insights into the thresholds that can lead to successful and safe burns. The next natural step of this work would be to conduct a set of fire experiments at the field scale under marginal conditions where this article could be considered as a useful guideline for such future experimental studies.

Author Contributions

"Conceptualization, Carmen Awad, Nicolas Frangieh, Thierry Marcelli and Jean Louis Rossi; methodology, Carmen Awad, Nicolas Frangieh, Thierry Marcelli and Jean Louis Rossi; software, Carmen Awad; validation, all the authors; formal analysis, all the authors; writing—original draft preparation, Carmen Awad, Nicolas Frangieh; writing—review and editing, all the authors; supervision, Thierry Marcelli

and Jean Louis Rossi. All authors have read and agreed to the published version of the manuscript."

Funding

This work was funded by the Corsican Region and the French state in the framework of the collaborative project GOLIAT (CPER: 40031).

Declaration of competing interest

"The authors declare no conflict of interest". "The funders had no role in the design of the study; in the collection, analyses, or interpretation of data; in the writing of the manuscript, or in the decision to publish the results".

Acknowledgements

All persons who have made substantial contributions to the work reported in the manuscript (e.g., technical help, writing and editing assistance, general support), but who do not meet the criteria for authorship, are named in the Acknowledgements and have given us their written permission to be named. If we have not included an Acknowledgements, then that indicates that we have not received substantial contributions from non-authors.

References

[1] D.D. Wade, J.D. Lunsford, A guide for prescribed fire in southern forests, Tech. Publ. R8-TP11 (1989).

[2] A.A. Brown, K.P. Davis, Forest Fire: Control and Use, second ed., McGraw-Hill Book Company, New-York, USA, 1973.

[3] R. Rachmawati, M. Ozlen, K.J. Reinke, J.W. Hearne, An optimisation approach for fuel treatment planning to break the connectivity of high-risk regions, For. Ecol. Manage. 368 (2016) 94–104, https://doi.org/10.1016/j.foreco.2016.03.014.

[4] J.K. Agee, C.N. Skinner, Basic principles of forest fuel reduction treatments, For. Ecol. Manage. 211 (2005) 83–96, https://doi.org/10.1016/j.foreco.2005.01.034.

[5] J.G. Cawson, T.J. Duff, Forest fuel bed ignitability under marginal fire weather conditions in Eucalyptus forests, Int. J. Wildland Fire 28 (2019) 198–204, https://doi.org/10.1071/WF18070.

[6] Nwcg, NWCG Smoke Management Guide for Prescribed Fire, 2018.

[7] K.L. Clark, W.E. Heilman, N.S. Skowronski, M.R. Gallagher, E. Mueller, R. M. Hadden, A. Simeoni, Fire behavior, fuel consumption, and turbulence and energy exchange during prescribed fires in pitch pine forests, Atmosphere 11 (2020) 1–24, https://doi.org/10.3390/atmos11030242.

[8] J.K. Hiers, J.J.O. Brien, J.M. Varner, B.W. Butler, M. Dickinson, J. Furman, M. Gallagher, D. Godwin, S.L. Goodrick, S.M. Hood, A. Hudak, L.N. Kobziar, R. Linn, E.L. Loudermilk, S. McCaffrey, K. Robertson, E.M. Rowell, N. Skowronski, A.C. Watts, K.M. Yedinak, Prescribed fire science : the case for a refined research agenda, Fire Ecol 16 (2020) 15, https://doi.org/10.1186/s42408-020-0070-8.

[9] R.C. Rothermel, A Mathematical Model for Predicting Fire Spread in Wildland Fuels, USDA Forest Service, Ogden, Utah, 1972. Research Paper INT-115, Intermountain Forest and Range Experiment Station, http://www.snap.uaf.edu/webshared/JenNorthway/AKFireModelingWorkshop/AKFireModelingWkshp/FSProAnalysis Guide References/Rothermel 1972 INT-115.pdf.

[10] Indiana division of Fish & Wildlife, Prescribed Burning Habitat Management Fact Sheet, 2005. www.wildlife.in.gov.

[11] T.A. Waldrop, S.L. Goodrick, Introduction to Prescribed Fire in Southern Ecosystems Southern Research Station, Asheville, 2018, 28804, www.srs.fs.usda.gov.

[12] J. Russell-Smith, A.C. Edwards, K.K. Sangha, C.P. Yates, M.R. Gardener, Challenges for prescribed fire management in Australia, Int. J. Wildland Fire (2019), https://doi.org/10.1071/WF18127.

[13] D. Morvan, Wind effects, unsteady behaviors, and regimes of propagation of surface fires in open field, Combust. Sci. Technol. 186 (2014) 869–888, https://doi.org/10.1080/00102202.2014.885961.

[14] T.A. Waldrop, S.L. Goodrick, Introduction to Prescribed Fire in Southern Ecosystems, Sci. Updat. SRS-054 - United States Dep. Agric, 2012, p. 80. www.srs.fs.usda.gov. (Accessed 26 August 2020).

[15] D.R. Weise, X. Zhou, L. Sun, S. Mahalingam, Fire spread in chaparral - "go or no-go? Int. J. Wildland Fire 14 (2005) 99–106, https://doi.org/10.1071/WF04049.

[16] J.B. Marsden-Smedley, W.R. Catchpole, A. Pyrke, Fire modelling in Tasmanian buttongrass moorlands. IV * Sustaining versus non-sustaining fires, Int. J. Wildland Fire 10 (2001) 255–262, https://doi.org/10.1071/WF01026.

[17] S. Leonard, Predicting sustained fire spread in tasmanian native grasslands, Environ. Manage. 44 (2009) 430–440, https://doi.org/10.1007/s00267-009-9340-6.

[18] D. Morvan, Numerical study of the effect of fuel moisture content (FMC) upon the propagation of a surface fire on a flat terrain, Fire Saf. J. 58 (2013) 121–131, https://doi.org/10.1016/j.firesaf.2013.01.010.

[19] R.M. Nelson, first ed., Academic Press, 2001 https://doi.org/10.1016/B978-012386660-8/50006-4 (Chapter 4) - Water Relations of Forest Fuels.

[20] C.G. Rossa, The effect of fuel moisture content on the spread rate of forest fires in the absence of wind or slope, Int. J. Wildland Fire 26 (2017) 24–31, https://doi.org/10.1071/WF16049.

[21] A.L. Sullivan, A review of wildland fire spread modelling , 3 : mathematical analogues and simulation models, Int. J. Wildland Fire 18 (2009) 387–403, https://doi.org/10.1071/WF06144.

[22] G.M. Davies, C.J. Legg, Fuel moisture thresholds in the flammability of calluna vulgaris, Fire Technol. 47 (2011) 421–436, https://doi.org/10.1007/s10694-010-0162-0.

[23] J.G. Goldammer, C. De Ronde (Eds.), Wildland Fire Management Handbook for Sub-sahara Africa, Global Fire Monitoring Center, 2004. http://www.fire.uni-freiburg.de/latestnews/GFMC-Wildland-Fire-Management-Handbook-Sub-Sahara-Africa-2004.pdf%0Ahttp://books.google.com/books?hl=en&lr=&id=WmrvZqAB2UEC&oi=fnd&pg=PR9&dq=Wildland+Fire+Management+Handbook+for+Sub-Sahara+Af.

[24] H.E. Anderson, R.C. Rothermel, Influence of moisture and wind upon the characteristics of free-burning fires, Symp. Combust. 10 (1965) 1009–1019, https://doi.org/10.1016/S0082-0784(65)80243-0.

[25] A. Pompe, R.G. Vines, The influence OF moisture ON the combustion OF leaves, Aust. For. 30 (1966) 231–241, https://doi.org/10.1080/00049158.1966.10675417.

[26] G.M. Byram, Combustion of Forest Fuels, in: K.P. Davis (Ed.), Forest Fire: Control and Use, New York McGraw Hill, 1959, pp. 61–89.

[27] N.K. King, The influence of water vapour on the emission spectra of flames, Combust. Sci. Technol. 6 (1973) 247–256, https://doi.org/10.1080/00102207308952327.

[28] J.-H. Balbi, D.X. Viegas, C. Rossa, J.-L. Rossi, F.-J. Chatelon, D. Cancellieri, A. Simeoni, T. Marcelli, Surface fires: No wind, No slope, marginal burning, J. Environ. Sci. Eng. A. 3 (2014) 73–86. https://hal.archives-ouvertes.fr/hal-01070946.

[29] R.A. Wilson, Observations of extinction and marginal burning states in free burning porous fuel beds, Combust. Sci. Technol. 44 (1985) 179–193, https://doi.org/10.1080/00102208508960302.

[30] L. Trabaud, Inflammabilite et combustibilite des principales especes des garrigues de la region mediterraneenne, Ecol. Plant. 11 (1976) 117–136 (accessed June 26, 2020), https://agris.fao.org/agris-search/search.do?recordID=US201303049599.

[31] J.P. Valdivieso, J. de D. Rivera, Effect of wind on smoldering combustion limits of moist pine needle beds, Fire Technol. 50 (2014) 1589–1605, https://doi.org/10.1007/s10694-013-0357-2.

[32] C. Awad, D. Morvan, J.-L. Rossi, T. Marcelli, F.J. Chatelon, F. Morandini, J.-H. Balbi, Fuel moisture content threshold leading to fire extinction under marginal conditions, Fire Saf. J. 118 (2020) 11, https://doi.org/10.1016/j.firesaf.2020.103226.

[33] D. Morvan, S. Méradji, G. Accary, Physical modelling of fire spread in Grasslands, Fire Saf. J. 44 (2009) 50–61, https://doi.org/10.1016/j.firesaf.2008.03.004.

[34] D. Morvan, Numerical study of the behaviour of a surface fire propagating through a firebreak built in a Mediterranean shrub layer, Fire Saf. J. 71 (2015) 34–48, https://doi.org/10.1016/j.firesaf.2014.11.012.

[35] D. Morvan, J.L. Dupuy, Modeling the propagation of a wildfire through a Mediterranean shrub using a multiphase formulation, Combust. Flame 138 (2004) 199–210, https://doi.org/10.1016/j.combustflame.2004.05.001.

[36] D. Morvan, Physical phenomena and length scales governing the behaviour of wildfires: a case for physical modelling, Fire Technol. 47 (2011) 437–460, https://doi.org/10.1007/s10694-010-0160-2.

[37] European Science & Technology Advisory Group, Evolving Risk of Wildfires in Europe - the Changing Nature of Wildfire Risk Calls for a Shift in Policy Focus from Suppression to Prevention, 2020. Brussels, Belgium, https://www.undrr.org/publication/evolving-risk-wildfires-europe-thematic-paper-european-science-technology-advisory.

[38] N. Frangieh, G. Accary, D. Morvan, S. Méradji, O. Bessonov, Wildfires front dynamics: 3D structures and intensity at small and large scales, Combust. Flame 211 (2020) 54–67, https://doi.org/10.1016/j.combustflame.2019.09.017.

[39] E. Pastor, L. Zárate, E. Planas, J. Arnaldos, Mathematical models and calculation systems for the study of wildland fire behaviour, Prog. Energy Combust. Sci. 29 (2003) 139–153, https://doi.org/10.1016/S0360-1285(03)00017-0.

[40] I. Sellami, B. Manescau, K. Chetehouna, C. de Izarra, R. Nait-Said, F. Zidani, BLEVE fireball modeling using Fire Dynamics Simulator (FDS) in an Algerian gas industry, J. Loss Prev. Process. Ind. 54 (2018) 69–84, https://doi.org/10.1016/j.jlp.2018.02.010.

[41] S. Rudz, K. Chetehouna, C. Strozzi, P. Gillard, Minimum ignition energy measurements for α-pinene/air mixtures, Combust. Sci. Technol. 186 (2014), https://doi.org/10.1080/00102202.2014.935604.

[42] A.M. Grishin, Mathematical Modeling of Forest Fires and New Methods of Fighting Them, Publishing House of the Tomsk University, Tomsk, Russia, 1997.

[43] A. Favre, L.S.G. Kavasznay, R. Dumas, J. Gaviglio, M. Coantic, La turbulence en mécanique des fluides : bases théoriques et expérimentales, méthodes statistiques, Gauthier-Villars, 1977.

[44] G. Cox, Combustion Fundamentals of Fire, Academic Press, 1995.

[45] V. Yakhot, L.M. Smith, The renormalization group, the ϵ-expansion and derivation of turbulence models, J. Sci. Comput. 7 (1992) 35–61, https://doi.org/10.1007/BF01060210.

[46] S.A. Orszag, Introduction to Renormalization Group Modeling of Turbulence, in: Simul. Model. Turbul. Flows, Oxford University Press, Inc., New York, 1996.
[47] B.F. Magnussen, B.H. Hjertager, On Mathematical Modeling of Turbulent Combustion with Special Emphasis on Soot Formation and Combustion, in: Symp. Combust., 1977, pp. 719–729, https://doi.org/10.1016/S0082-0784(77)80366-4. Cambridge, Massachusetts.
[48] K.J. Syed, C.D. Stewart, J.B. Moss, Modelling soot formation and thermal radiation in buoyant turbulent diffusion flames, Symp. Combust. (1991) 1533–1541, https://doi.org/10.1016/S0082-0784(06)80423-6.
[49] J. Nagle, R.F. Strickland-Constable, Oxidation of Carbon between 1000–2000°C, in: Proc. Fifth Conf. Carbon, Pergamon Press, 1962, pp. 154–164, https://doi.org/10.1016/b978-0-08-009707-7.50026-1.
[50] D. Morvan, S. Méradji, G. Accary, Physical modelling of fire spread in Grasslands, Fire Saf. J. 44 (2009) 50–61, https://doi.org/10.1016/j.firesaf.2008.03.004.
[51] F.P. Incropera, D.P. DeWitt, Fundamentals of heat and mass transfer. https://doi.org/10.1016/j.applthermaleng.2011.03.022, 1996.
[52] R.H. Shaw, G. Den Hartog, H.H. Neumann, Influence of foliar density and thermal stability on profiles of Reynolds stress and turbulence intensity in a deciduous forest, Boundary-Layer Meteorol. 45 (1988) 391–409, https://doi.org/10.1007/BF00124010.
[53] S.V. Patankar, Numerical heat transfer and fluid flow. https://doi.org/10.13182/nse81-a20112, 1980.
[54] H.K. Versteeg, W. Malalasekera, An introduction to computational fluid dynamics - the finite volume method. http://scholar.google.com/scholar?hl=en&btnG=Search&q=intitle:Computational+fluid+dynamics.+The+basics+with+applications#6%5Cnhttp://scholar.google.com/scholar?hl=en&btnG=Search&q=intitle:Computational+Fluid+Dynamics:+The+Basics+with+Applications.+1995%23, 2007.
[55] B.P. Leonard, S. Mokhtari, Beyond first-order upwinding: the ultra-sharp alternative for non-oscillatory steady-state simulation of convection, Int. J. Numer. Methods Eng. 30 (1990) 729–766, https://doi.org/10.1002/nme.1620300412.
[56] M.F. Modest, Radiative Heat Transfer, Academic Press, 2003.
[57] P.J. Coelho, Numerical simulation of the interaction between turbulence and radiation in reactive flows, Prog. Energy Combust. Sci. 33 (2007) 311–383, https://doi.org/10.1016/j.pecs.2006.11.002.
[58] D. Morvan, J.L. Dupuy, Modeling of fire spread through a forest fuel bed using a multiphase formulation, Combust. Flame 127 (2001), https://doi.org/10.1016/S0010-2180(01)00302-9, 1981–1994.
[59] D. Morvan, S. Meradji, G. Accary, Wildfire behavior study in a mediterranean pine stand using a physically based model, Combust. Sci. Technol. 180 (2008) 230–248, https://doi.org/10.1080/00102200701600978.
[60] A.C. Fernandez-Pello, S.R. Ray, I. Glassman, Downward flame spread in an opposed forced flow, Combust. Sci. Technol. 19 (1978) 19–30, https://doi.org/10.1080/00102207808946860.
[61] J. Gould, Validation of the Rothermel fire spread model and related fuel parameters in grassland fuels, Proc. Conf. Bushfire Model. Fire Danger Rat. Syst. (1991) 51–64.
[62] A. Ranganathan, The levenberg-marquardt algorithm, Tutoral LM Algorithm 11 (2004) 101–110.
[63] P.L. Andrews, BEHAVE: Fire Behavior Prediction and Fuel Modeling System - BURN Subsystem, vol. 1, Part, Ogden, UT 84401, 1986.
[64] N.J. De Mestre, E.A. Catchpole, D.H. Anderson, R.C. Rothermel, Uniform propagation of a planar fire front without wind, Combust. Sci. Technol. 65 (1989) 231–2444, https://doi.org/10.1080/00102208908924051.